PAPER ID: 146
DOI: 10.18462/iir.rankine.2020.146

Performance Prediction and Optimisation of Twin-Screw Expander

Kisorthman VIMALAKANTHAN[(1)], Matthew READ[(2)], Ahmed KOVACEVIC[(3)]

[(1, 2, 3)] City, University of London
London, EC1V 0HB, United Kingdom,
[1]k.vimalakanthan@city.ac.uk, [2]m.read@city.ac.uk, [3]a.kovacevic@city.ac.uk

ABSTRACT

Positive displacement machines have been identified as appropriate expanders for small scale power generation systems such as ORCs. Screw expanders can operate with good efficiency for working fluids under both dry and two-phase conditions. Detailed understanding of the fluid expansion process is required to optimise the machine design and operation for specific applications, and accurate design tools are therefore essential. Using experimental data for R245fa expansion, both CFD and chamber models have been applied to investigate the accuracy of computed performances. Both models are shown to match experimental power output and mass flowrate with good accuracy. Finally, the validated chamber model is used to evaluate the maximum isentropic efficiency map for the chosen expander. This performance map can be used with ORC optimisation tools to identify deign built-in volume ratio of twin-screw expander and the required rotational speeds to operate at the maximum isentropic efficiency.

Keywords: twin screw, air, two phase, expander, performance, optimisation, chamber model, CFD, validation, built-in volume ratio.

1. INTRODUCTION

In recent years, substantial effort has been put into reducing global CO_2 emissions from industrial processes, which alone accounts for almost 26% (275 Mtoe/yr) of Europe's energy consumption (Panayiotou et al., 2017). Theoretical studies looking at global heat potential (Forman et al., 2016) have shown that around 52% of primary energy consumption is currently rejected as waste heat, with 63% of the global waste heat potential existing as low temperature heat source (<100 ºC). Organic Rankine Cycle (ORC) systems provide the means of extracting useful power from low temperature heat sources. The potential thermodynamic and economic benefits of ORC systems considering two-phase expansion are well reported within the literature (Fischer, 2011; Read et al., 2017). It is widely reported that for power outputs in the tens of kWs, screw expanders are considered a suitable technology among the volumetric machines (Öhman & Lundqvist, 2013; Bianchi et al., 2018). There are, however, significant challenges with achieving efficient two-phase expansion due to the large density changes involved, and optimisation of the machine design and operating conditions is essential.

The built-in volume ratio (ϵ_v), of a twin-screw expander is the ratio between the maximum volume of the working chamber and the volume at which the inlet port closes. This is related to machine geometry, and increasing ϵ_v reduces the inlet port area, limiting mass flow rate and efficiency when operating at large density ratios. Thus it is important to develop a validated numerical model that accurately captures the effect of volumetric expansion ratio on the expander efficiency. The study by Bianchi et al. (2018) presenting the numerical results of modelling two-phase expanders further highlights the paramount importance of validation against experimental data.

This paper presents the development of a validated 1D modelling tool for twin screw expanders operating over a range of fluid inlet conditions, based on a chamber model approach (Stosic et al., 2005). A detail validation case for single phase air is presented in (Vimalakanthan et al., 2020). In this study, results from the 1D chamber model and a more detailed 3D transient multiphase CFD model are compared against the experimental data for single and two-phase expansion of the refrigerant R245fa. Experimental measurements have previously been conducted using the expander described in Figure 1. Furthermore, using the validated 1D model a map

of maximum expander efficiency as a function of built-in volume ratio and inlet pressure is presented for two-phase operation.

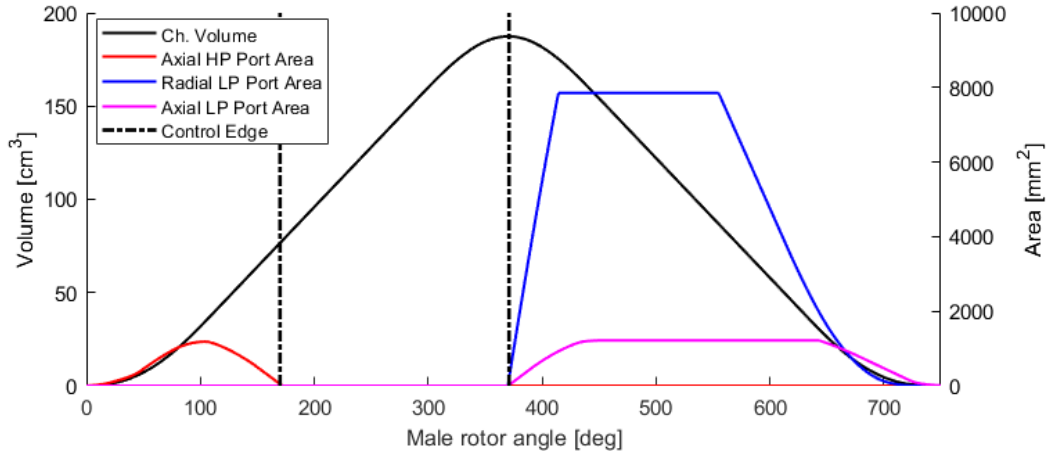

Figure 1: Port areas and volume curve of the investigated screw expander - $\epsilon_v = 2.4$, 4/5 male/female lobes, rotor length = 158mm, male rotor – [dia.= 102mm, wrap angle= 300deg], female rotor – [dia.= 80mm, wrap angle= 240deg], HP port: Axial only, LP port: Radial and Axial

2. MODELLING

This study develops and compares two numerical modelling approaches for twin-screw expanders. The first is a quasi 1D chamber model (1D Ch. Model), which is a computationally efficient approach to solve the system of equations. The second approach considers the expander in three-dimensional Computational Fluid Dynamics (3D CFD) numerical environment and solves the full Navier-Stokes equations with RANS k-e closure for turbulence modelling. Such an approach requires high computational efforts on high performance clusters. The in-house computational code SCORG© (Rane et al., 2019) enables use of both chamber modelling and 3D CFD in screw machines.

2.1. Chamber model (1D Ch. Model)

Based on the geometry calculation (Figure 1) from SCORG©, commercial software GT-SUITE™ was used to implement the chamber modelling approach previously outlined (Stosic et al., 2005). This software models the 1D formulation of the Navier-Stokes equations to model the fluid behaviour on a staggered grid spatial discretisation. The expander is divided into various fluid components (Figure 2) such that an inlet pipe connects to a manifold that feeds the working chambers of the expander. After expansion the fluid then enters another manifold and exits via the outlet piping. The pipe volumes are divided into sub volumes while the chamber and intake and exhaust manifolds are represented by a single volume where the scalar fluid properties are assumed to be uniform, while the vector variables are solved at the boundary.

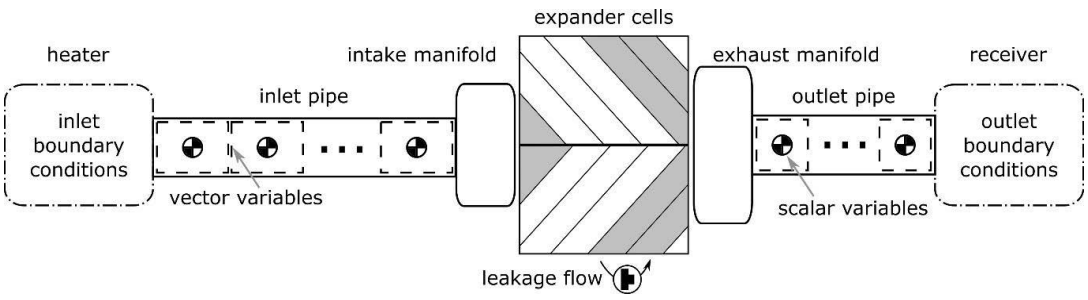

Figure 2: Modelling approach for 1D Ch. Model (Bianchi et al., 2018)

The chamber volume and the corresponding flow areas for ports and leakage paths are provided as a function of rotor angle (Figure 1). The current model assumes adiabatic walls. All fluid components within the 1D Ch.

Model including leakage flows are model as flow through an orifice. The systems of conservation equations are solved using explicit 5th order Runge-Kutta integration scheme to solve for mass and internal energy. With the known volume and mass, the corresponding density is calculated. The density and internal energy values are then used to determine the pressure and temperature via the NIST REFPROP database (Lemmon et al., 2010).

2.2. Computational Fluid Dynamics Model (3D CFD)

In order to assess the accuracy of the Chamber model discussed in the previous section, 3D transient CFD simulations were conducted. As the working fluid flows through the machine, the net force exerted by the fluid on the rotors causes rotation, with expansion of the fluid occurring once the inlet port closes (Figure 3a). This results in net power output via the shaft of the male rotor, which can be used to drive a mechanical load or electrical generator.

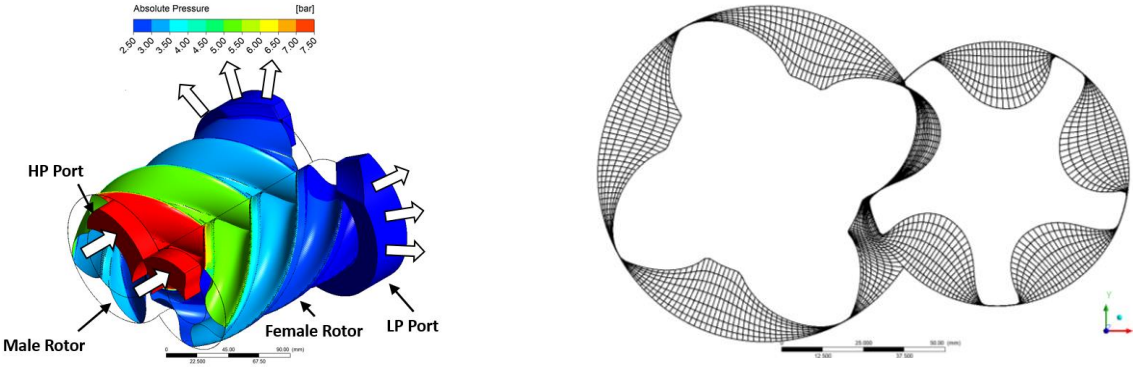

Figure 3: Pressure variation in twin screw expander and hexahedral grid adapted for the rotor domain

The computational fluid domain is decomposed into three main sub-domains, namely the high pressure (HP) port, rotor domain containing both the male and female rotors, and the low pressure (LP) port. Moreover, the end face clearances were modelled with additional domains attached on both sides of rotors. All domains were connected via non-conformal Generalised Grid Interface (GGI). The rotor domain is updated by importing the corresponding grid at each time intervals to model the rotation.

The whole expander flow domain is discretised with approximately 550,000 hexahedral elements. The rotor grid is modelled with 465,000 elements, containing 160, 7 and 180 divisions per rotor in the circumferential, radial and axial directions respectively (Figure 3b). A conformal interlobe region contains 50 divisions. The port domains were also modelled using hexahedral elements: 25,000 elements for HP port and 60,000 elements for the LP Port. The conformal computational grid for the rotor domain with the ports was generated using SCORG© (Rane et al., 2019). All CFD simulations were performed using the ANSYS CFX© solver.

3. RESULTS

The numerical simulations were conducted for several experimental conditions ranging from 6-12bar inlet pressure, and running at three different rotational speeds: 1500, 2000 and 2500RPM, for both saturated vapour ($x_{in} = 1$) and two phase ($x_{in} = 0.91$) expander inlet conditions. The experiment did not have the instrumentation implemented to measure the internal pressure readings from the expander, thus only the shaft power and mass flow rate data from the experiment is used to validate the numerical models. In order to make comparison with the shaft power measurements, a constant 80% mechanical efficiency is assumed on the computed indicated power values.

Clearance gaps for the investigated expander were set at a nominal 50um for all gaps including interlobe, radial and axial. Due to mechanical and thermal loads these clearance gaps are known to change in operation. Operational clearance settings of 100x100x50x200um corresponding to the interlobe, radial, HP end face and LP end face were chosen for both 3D CFD and 1D Ch. Model simulations.

3.1. Validation Results

The results from both 3D CFD and Chamber model agree well with the measured shaft power and mass flow rate for 1500 and 2000 RPM rotational speed. At higher rotational speed of 2500 RPM, both 3D CFD and Chamber models over predicts the shaft power within 5 and 10% respectively. However, this error in shaft power comparison at higher rotation speed is expected to be due to the lack of information regarding the mechanical losses. The considered 80% mechanical efficiency for all rotational speeds may not be suitable, where the bearing losses are expected to scale with RPMs in a quadratic relationship. Further information regarding the mechanical losses is required to assess the quality of the comparison at larger RPMs.

The 3D CFD model consistently over predicts the mass flow rate by 7.5% while the Chamber model matches the measured mass flow rates very closely for all speeds. Nevertheless, both numerical models predict the expander mass flow rates within the experimental errors.

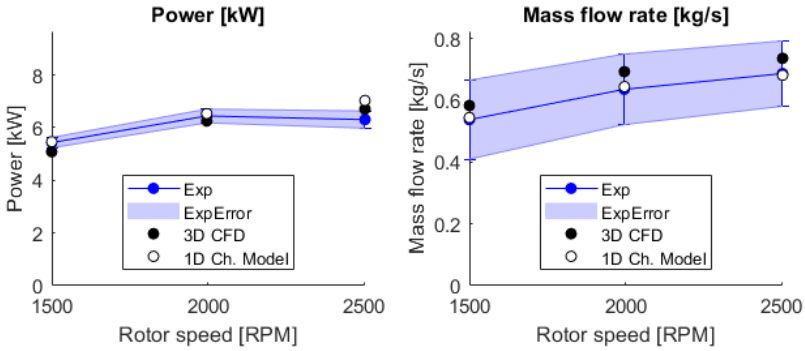

Figure 4: Expander shaft power and mass flow rate against rotor speed, $\epsilon_v = 2.4$, clearance (interlobe, radial, HP and LP End face): 100x100x50x200um, Pi= 7.5[bar], $x_{in} = 0.91$.

Comparing the internal pressures from both numerical models (Figure 5), the 3D CFD model predicts a larger drop in pressure during the expansion process than occurs in the Chamber model. There is no significant difference in fluid conditions at the point when the inlet port closes, and it can also be seen that the difference in the internal pressures reduces with increasing the rotational speeds. This is an indication that these two numerical models calculate significantly different leakage flows; the higher leakage calculated by the 3D CFD model reduces the mass contained in a working chamber, and hence the pressure, during expansion. As the relative leakage flows reduce with increase in rotational speed in both models, it is shown that the difference in the calculated pressures is reduced.

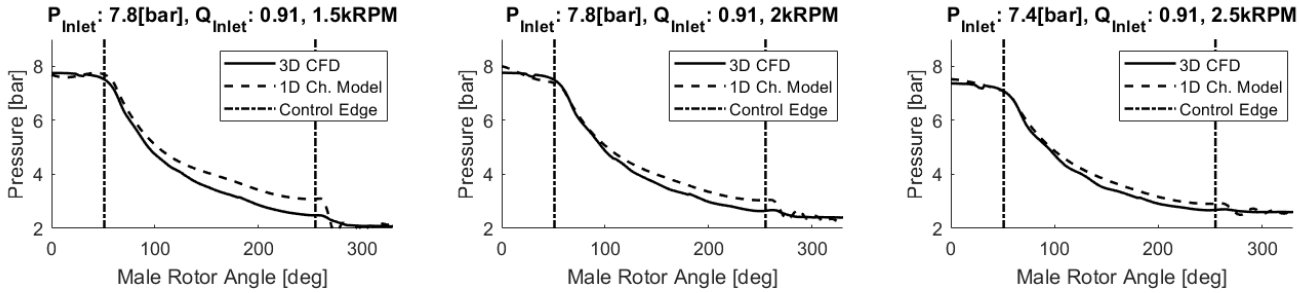

Figure 5: Expander's indicated pressure against male rotor angle for different RPMs, $\epsilon_v = 2.4$, clearance (interlobe, radial, HP and LP End face): 100x100x50x200um, Pi= 7.5[bar], $x_{in} = 0.91$.

The results at 2000 RPM for different inlet pressures at single and two phase conditions (Figure 6 and Figure 7) show that both models predict the power and mass flow rates with good accuracy compared to measurements. The 3D CFD model consistently under predicts the shaft power, while the Chamber model results match closely with experiment.

Comparing the mass flow rates at these conditions (Figure 7) shows that both numerical models are able to archive results that are within the experimental error. However it is noted that the Chamber model shows better

agreement with measurements for two-phase compared to single phase conditions. The Chamber model under predicts the power outputs for inlet pressures above 8bar. The 3D CFD model on the other hand over predicts the mass flow rate but the trends are same as in experiment for both single and two-phase conditions.

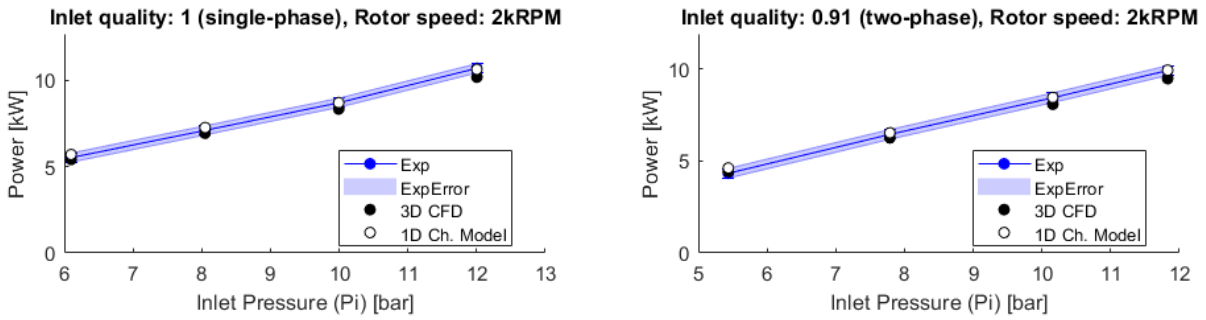

Figure 6: Expander shaft power for different inlet pressures at single and two-phase conditions, $\epsilon_v = 2.4$, clearance (interlobe, radial, HP and LP End face): 100x100x50x200um, 2000RPM.

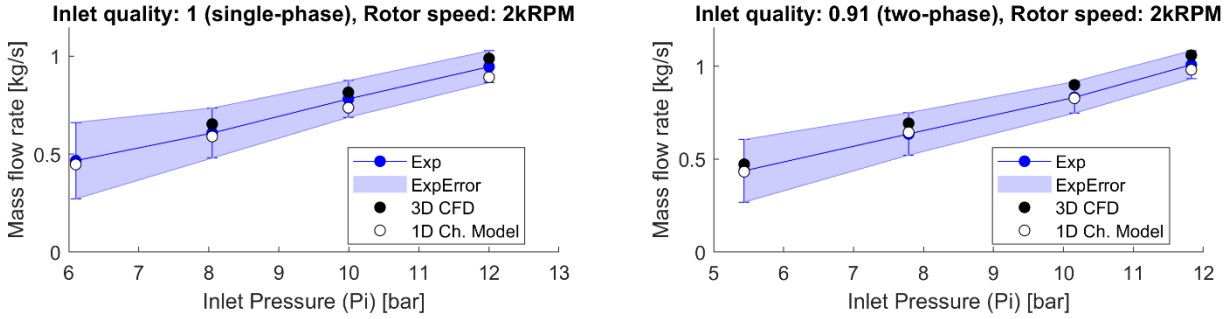

Figure 7: Expander mass flow rate for different inlet pressures at single and two-phase conditions, $\epsilon_v = 2.4$, clearance (interlobe, radial, HP and LP End face): 100x100x50x200um, 2000RPM

3.2. Maximum Efficiency maps

In general, the isentropic efficiency of a twin screw expanders depends on the built-in volume ratio (ϵ_v), volumetric expansion ratio and rotational speed. The built-in volume ratio is a function of the HP port geometry, while the volumetric expansion ratio is based on the inlet and outlet condition. These two parameters determine the expanders' ability to match the expansion occurring within the machine to the application. At higher rotational speeds the leakage become a lower proportion of the mass flow rate, resulting in higher maximum isentropic efficiency when operating with a suitable value of ϵ_v.

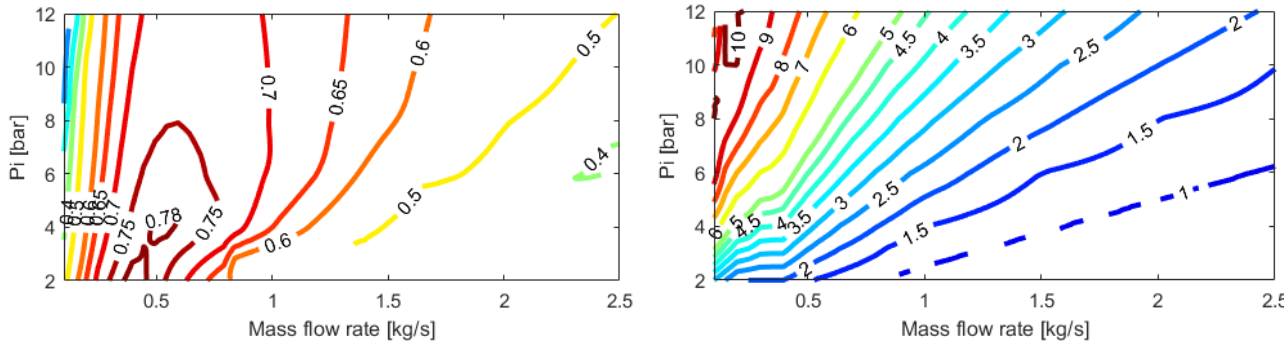

Figure 8: Maximum efficiency map and its corresponding value of built-in volume ratio (ϵ_v), $x_{in} = 0.91$, $P_{out} =$ 1bar

Using the established Chamber model, this study was conducted to evaluate the maximum isentropic efficiency map for the chosen expander considering two-phase inlet conditions with $x_{in} = 0.91$, $p_{in} = 1 - 12$bar, $\epsilon_v = 1 - 10$, and rotational speeds of 500-5000 RPM. All simulations were conducted with an outlet pressure of 1bar. The resulting performance map illustrates how ORC optimisation tools can be developed to identify the best combination of machine size, port geometry and operational speed for twin screw expander applications.

The maximum efficiency map and its corresponding ϵ_v requirement are shown in Figure 8. For any mass flowrate higher than 0.35kg/s the optimum rotational speed required for maximum efficiency was at 5000 RPM, for lower mass flowrates the optimum rotational speed linearly increases from 500 RPM. Based on these results, the optimum performance of the chosen expander considering the specified two-phase R245fa inlet condition ($x_{in} = 0.91$) is achieved when supplying 0.5kg/s at 4bar and running the machine at 5000 RPM, as shown in Figure 8. Higher mass flow rate and power output can only be achieved by reducing the built-in volume ratio, leading to lower expander efficiency.

4. CONCLUSIONS

Using experimental data for R245fa expansion, both CFD and chamber models have been applied to investigate the accuracy of computed performances of twin screw expanders. Both models showed a good match with experimentally obtained power output and mass flowrate. The maximum efficiency map for a two-phase inlet condition have been successfully generated for the chosen expander design, which can be used with ORC optimisation tool to evaluate ideal operating conditions. In future work, this study will be extended to various two-phase conditions ($0.3 < x_{in} < 0.9$) to establish a larger domain space for evaluating maximum efficiency.

REFERENCES

Bianchi, G., Kennedy, S., Zaher, O., Tassou, S.A., Miller, J., & Jouhara, H. (2018). Numerical modelling of a twophase twin-screw expander for trilateral flash cycle applications. *International Journal of Refrigeration*, In-press. doi: https://doi.org/10.1016/j.ijrefrig.2018.02.001.

Fischer, J. (2011). Comparison of trilateral cycles and organic Rankine cycles. *Energy*, 36, 6208-6219.

Forman, C., Muritala, I.K., Pardemann, R. and Meyer, B., 2016. Estimating the global waste heat potential. *Renewable and Sustainable Energy Reviews*, 57, pp.1568-1579.

Hütker, J. and Brümmer, A., 2013, September. Physics of a dry running unsynchronized twin screw expander. *In Proceedings of the 8th International Conference on Compressors and their Systems*, London, UK (pp. 9-10).

Lemmon, E.W., Huber, M.L. and McLinden, M.O., 2010. NIST Standard Reference Database 23, Reference Fluid Thermodynamic and Transport Properties (REFPROP), version 9.0, *National Institute of Standards and Technology*. p.2010.

Öhman, H., & Lundqvist, P., (2013). Experimental investigation of a Lysholm Turbine operating with superheated, saturated and 2-phase inlet conditions. *Applied Thermal Engineering*, 50, 1211–1218.

Panayiotou, G.P., Bianchi, G., Georgiou, G., Aresti, L., Argyrou, M., Agathokleous, R., Tsamos, K.M., Tassou, S.A., Florides, G., Kalogirou, S. and Christodoulides, P., 2017. Preliminary assessment of waste heat potential in major European industries. *Energy Procedia*, 123, pp.335-345.

Read, M. G., Smith, I. K., & Stosic, N. (2017). Optimisation of power generation cycles using saturated liquid expansion to maximise heat recovery. *P I Mech Eng E-J Pro*, 231(1), 57-69.

Rane, S., Kovačević, A. and Stošić, N., 2019. Grid Generation for CFD Analysis and Design of a Variety of Twin Screw Machines. *Designs*, 3(2), p.30.

Stosic, N., Smith, I.K. and Kovacevic, A., 2005. Calculation of Screw Compressor Performance. *Screw Compressors: Mathematical Modelling and Performance Calculation*, pp.49-75.

Vimalakanthan, K., Read, M. G., & Kovacevic, A. (2020), Numerical Modelling and Experimental Validation of Twin-Screw Expander, *25th International Compressor Engineering Conference at Purdue*, July 13-16, Paper 1332